PROOF COVER SHEET

Author(s):	Salvatore Maurizio Tredici, Alessandro Buccolieri, Luciano Tanini, Matteo Calcagnile, Daniela Manno, and Pietro Alifano
Article title:	Calcite-forming *Bacillus licheniformis* Thriving on Underwater Speleothems of a Hydrothermal Cave
Article no:	UGMB_A_1476626
Enclosures:	1) Query sheet 2) Article proofs

Dear Author,

1. Please check these proofs carefully. It is the responsibility of the corresponding author to check these and approve or amend them. A second proof is not normally provided. Taylor & Francis cannot be held responsible for uncorrected errors, even if introduced during the production process. Once your corrections have been added to the article, it will be considered ready for publication.

Please limit changes at this stage to the correction of errors. You should not make trivial changes, improve prose style, add new material, or delete existing material at this stage. You may be charged if your corrections are excessive (we would not expect corrections to exceed 30 changes).

For detailed guidance on how to check your proofs, please paste this address into a new browser window: http://journalauthors.tandf.co.uk/production/checkingproofs.asp

Your PDF proof file has been enabled so that you can comment on the proof directly using Adobe Acrobat. If you wish to do this, please save the file to your hard disk first. For further information on marking corrections using Acrobat, please paste this address into a new browser window: http://journalauthors.tandf.co.uk/production/acrobat.asp

2. Please review the table of contributors below and confirm that the first and last names are structured correctly and that the authors are listed in the correct order of contribution. This check is to ensure that your name will appear correctly online and when the article is indexed.

Sequence	Prefix	Given name(s)	Surname	Suffix
1		Salvatore Maurizio	Tredici	
2		Alessandro	Buccolieri	
3		Luciano	Tanini	
4		Matteo	Calcagnile	
5		Daniela	Manno	
6		Pietro	Alifano	

Queries are marked in the margins of the proofs, and you can also click the hyperlinks below.

General points:

1. **Permissions:** You have warranted that you have secured the necessary written permission from the appropriate copyright owner for the reproduction of any text, illustration, or other material in your article. Please see http://journalauthors.tandf.co.uk/permissions/usingThirdPartyMaterial.asp.

2. **Third-party content:** If there is third-party content in your article, please check that the rightsholder details for re-use are shown correctly.

3. **Affiliation:** The corresponding author is responsible for ensuring that address and email details are correct for all the co-authors. Affiliations given in the article should be the affiliation at the time the research was conducted. Please see http://journalauthors.tandf.co.uk/preparation/writing.asp.

4. **Funding:** Was your research for this article funded by a funding agency? If so, please insert `This work was supported by <insert the name of the funding agency in full>', followed by the grant number in square brackets `[grant number xxxx]'.
5. **Supplemental data and underlying research materials:** Do you wish to include the location of the underlying research materials (e.g. data, samples or models) for your article? If so, please insert this sentence before the reference section: `The underlying research materials for this article can be accessed at <full link>/ description of location [author to complete]'. If your article includes supplemental data, the link will also be provided in this paragraph. See <http://journalauthors.tandf.co.uk/preparation/multimedia.asp> for further explanation of supplemental data and underlying research materials.

6. The **PubMed** (http://www.ncbi.nlm.nih.gov/pubmed) and **CrossRef databases** (www.crossref.org/) have been used to validate the references. Changes resulting from mismatches are tracked in red font.

AUTHOR QUERIES

Q1: Reference "Parkhurst et al. (1995)" has been changed to "Parkhurst (1995)" to match the reference list. Please check.
Q2: Please provide complete details for (Wei et al. 2015) in the reference list or delete the citation from the text.
Q3: A disclosure statement reporting no conflict of interest has been inserted. Please correct if this is inaccurate.
Q4: There is no mention of (Brown 1994) in the text. Please insert a citation in the text or delete the reference as appropriate.

How to make corrections to your proofs using Adobe Acrobat/Reader

Taylor & Francis offers you a choice of options to help you make corrections to your proofs. Your PDF proof file has been enabled so that you can mark up the proof directly using Adobe Acrobat/Reader. This is the simplest and best way for you to ensure that your corrections will be incorporated. If you wish to do this, please follow these instructions:

1. Save the file to your hard disk.

2. Check which version of Adobe Acrobat/Reader you have on your computer. You can do this by clicking on the Help" tab, and then About".

If Adobe Reader is not installed, you can get the latest version free from http://get.adobe.com/reader/.

3. If you have Adobe Acrobat/Reader 10 or a later version, click on the Comment" link at the right-hand side to view the Comments pane.

4. You can then select any text and mark it up for deletion or replacement, or insert new text as needed. Please note that these will clearly be displayed in the Comments pane and secondary annotation is not needed to draw attention to your corrections. If you need to include new sections of text, it is also possible to add a comment to the proofs. To do this, use the Sticky Note tool in the task bar. Please also see our FAQs here: http://journalauthors.tandf.co.uk/production/index.asp.

5. Make sure that you save the file when you close the document before uploading it to CATS using the Upload File" button on the online correction form. If you have more than one file, please zip them together and then upload the zip file.
If you prefer, you can make your corrections using the CATS online correction form.

Troubleshooting

Acrobat help: http://helpx.adobe.com/acrobat.html
Reader help: http://helpx.adobe.com/reader.html

Please note that full user guides for earlier versions of these programs are available from the Adobe Help pages by clicking on the link Previous versions" under the Help and tutorials" heading from the relevant link above. Commenting functionality is available from Adobe Reader 8.0 onwards and from Adobe Acrobat 7.0 onwards.

Firefox users: Firefox's inbuilt PDF Viewer is set to the default; please see the following for instructions on how to use this and download the PDF to your hard drive: http://support.mozilla.org/en-US/kb/view-pdf-files-firefox-without-downloading-them#w_using-a-pdf-reader-plugin

GEOMICROBIOLOGY JOURNAL
https://doi.org/10.1080/01490451.2018.1476626

Calcite-forming *Bacillus licheniformis* Thriving on Underwater Speleothems of a Hydrothermal Cave

Salvatore Maurizio Tredici[a]*, Alessandro Buccolieri[a]*, Luciano Tanini[b], Matteo Calcagnile[a], Daniela Manno[c] and Pietro Alifano[a]

[a]Department of Biological and Environmental Sciences and Technologies, University of Salento, Lecce, Italy; [b]Grotta Giusti Diving, Monsummano Terme, Italy; [c]Department of Mathematics and Physics "Ennio De Giorgi", University of Salento, Lecce, Italy

ABSTRACT

The underwater environment of Grotta Giusti (Monsummano Terme, Italy) is a suggestive setting with different types of speleothems including "leafy" and "cauliflower" concretions along the walls and roof, and conical pseudo-stalagmites on the floor. Very high calcium and dissolved CO_2 levels, and massive calcium carbonate precipitation characterize this cave environment. Yet, life thrives on the leafy concretion surfaces with loads of cultivable heterotrophic microorganisms around 10^5 colony-forming units per cm^2. *Bacillus licheniformis* appeared to be the prevalent cultivable microorganism on a low-nutrient medium that was used for screening. 16S rRNA gene-based polymerase chain reaction–single strand conformation polymorphism profiling indicated that Group VI *Bacillaceae* species was well represented in the bacterial community of underwater speleothems. Interpretation of X-ray diffraction spectra and Raman spectroscopy data indicated that the *B. licheniformis* isolate produced *in vitro* abundant calcite microcrystals that were also characterized by scanning electron microscopy coupled with energy dispersive X-ray spectroscopy. Production of calcite microcrystals was analyzed in different media (Christensen's urea agar and B4 calcium carbonate precipitation medium) and incubation conditions, and it was found to be enhanced by nitrate supplement in B4 medium under low-oxygen conditions. B4 and B4-nitrate media also stimulated antibiotic production by the *B. licheniformis* isolate, which was analyzed by microbiological assays.

ARTICLE HISTORY
Received 16 May 2017
Accepted 7 May 2018

KEYWORDS
Bacillus licheniformis; calcite biomineralization; Raman spectroscopy; SEM-EDX; XRD

Introduction

Grotta Giusti (Monsummano Terme, Tuscany, Italy) is a hydrothermal karst cave and a major Italian spa center, which takes its name from the owners of the local limestone quarry (Piciocchi and Utili 1976). The cave intersects with a thermal aquifer flowing some feet from the surface, and was discovered by chance in the spring of 1849 by some quarry workers. After removing the stones that covered the roof of the quarry, they found themselves facing a vast underground cavity (the third largest shallow hydrothermal cave in Europe) with the presence of lakes, winding corridors, stalactites, and stalagmites. The most typical feature in this setting is a multitude of domes or hollow half-spheres in the roof and walls, which were generated by strong convection process that is promoted by high air temperature gradient (the surface water temperature of the lake inside the cave ranges around 32–34 °C while the rock wall at the upper levels is below 20 °C), and by high concentration of CO_2 in the underground lakes, in the air and in the water condensing on the roof and walls (Cigna and Forti 1986).

In the early 1980s, by exploring the underwater part of the Grotta Giusti some divers discovered an impressive setting with different types of speleothems including "leafy" and "cauliflower" concretions along the walls and roof, and conical pseudo-stalagmites (also known as subaqueous gravitational cones) on the floor, which are formed by underwater accumulations of the calcite crystals that float on the surface of the thermal water in the various underground lakes (Piccini 2000). The purpose of this study was to characterize cultivable bacteria living on the surface of the submerged concretions of the Grotta Giusti to provide some insight on their adaptive mechanisms to this cave environment that is characterized by very high calcium and dissolved CO_2 levels, and on their possible contribution in speleothem accretion. Indeed, although the growth of speleothems such as stalactites and stalagmites by calcite precipitation has commonly been considered as an abiogenic process (Broughton 1983a, b, c; Kendall and Broughton 1978), there is a well-documented involvement of microorganisms in speleothem formation and/or accretion (Baskar et al. 2005, 2006, 2007, 2009; Cacchio et al. 2004; Jones 2001, 2010;

CONTACT Pietro Alifano pietro.alifano@unisalento.it Department of Biological and Environmental Sciences and Technologies, University of Salento, Via provinciale Lecce-Monteroni, 73100 Lecce, Italy
*These authors contributed equally to this work.
Color versions of one or more of the figures in the article can be found online at www.tandfonline.com/ugmb.
Supplemental data for this article can be accessed here.

Forti 2002; Mulec et al. 2007; Pacton et al. 2013), and this role may be critical in the case of submerged speleothems.

Calcium carbonate precipitation may occur by two different mechanisms as either biologically controlled or biologically induced phenomenon. The first one is carried out only by several microorganisms that use specific metabolic pathways to control the process (Benzerara et al. 2011; Bazylinski and Moskowitz 1997). The second one is much more common, involves numerous bacterial species in different environments, such as soils, freshwaters, oceans and saline lakes, and is associated with microbial surface structures and several metabolic activities. In this case, the types of minerals produced are mainly dependent on the environmental conditions (Benzerara et al. 2011; Boquet et al. 1973; Brennan et al. 2004; Douglas and Beveridge 1998; Zamarreño et al. 2009). Indeed, calcium carbonate has three polymorphs: calcite, aragonite and vaterite. Calcite and aragonite are the most common biologically formed polymorphs, while vaterite is not commonly found because it is less stable (Rodriguez-Navarro et al. 2007, 2012; Tourney and Ngwenya 2009). Calcite is more stable than aragonite at standard atmospheric temperature and pressure, while aragonite is more stable in high-pressure environments, although aragonite can be formed at atmospheric pressure in certain conditions, such as hot springs. In particular, the presence of other doubly charged ions, such as Mg^{2+}, seems to favor the formation of aragonite (Falini et al. 1996). As a consequence, biologically induced calcium carbonate polymorph and crystal morphology mostly depend on the environment in which bacteria dwell in addition to the expression of specific bacterial surface structures that may be crucial for the crystallization process (González-Muñoz et al. 2010; Rodriguez-Navarro et al. 2012).

A variety of microbial metabolic processes have been known to induce carbonate precipitation including photosynthetic carbon fixation, ureolysis, denitrification, ammonification, sulfate reduction, anaerobic sulfide oxidation, and methane oxidation by increasing pH in the microenvironment around cells and/or dissolved carbon dioxide concentration (Knorre and Krumbein 2000; Zhu and Dittrich 2016). Moreover, microbial surfaces are favorable sites for calcium carbonate nucleation by providing negatively charged carboxyl, phosphate and amines that adsorb Ca^{2+} (Zhu and Dittrich 2016). Extracellular polymeric substances (EPSs) in microbial biofilms can trap and bind considerable amounts of calcium thereby facilitating calcium carbonate precipitation (Arp et al. 1999; Braissant et al. 2007; Dupraz and Visscher 2005; Mobley and Hausinger 1989).

Among the nitrogen compound metabolic processes that induce carbonate precipitation, one of the most effective is urea hydrolysis that produces carbonate and ammonia, increasing locally the pH and carbonate concentration (Anbu et al. 2016; Fujita et al. 2000; Hammes et al. 2003; Phillips et al. 2013). This process is rather common because urea is utilized as a nitrogen source by a variety of microorganisms including Fungi, Proteobacteria, Firmicutes, Actinomycetes, and Cyanobacteria (Hasan 2000). Among Firmicutes, the order Bacillales comprises many ureolytic species including *Sporosarcina pasteurii*, *Bacillus lentus*, *Bacillus sphericus*, *Bacillus diminuta*, and *Bacillus subtilis* (Hasan 2000). Both cellular respiration and urea decomposition provide a source of carbon dioxide. In addition to urease, another enzyme that facilitates calcium carbonate precipitation is carbonic anhydrase that catalyzes the rapid inter-conversion of carbon dioxide and water to bicarbonate and protons (Achal and Pan 2011; Botré and Botré 1989). A synergistic role of bacterial urease and carbonic anhydrase in carbonate mineralization has been proposed (Dhami et al. 2014).

The denitrification process may also induce calcium carbonate precipitation by increasing the pH in the surrounding environment, and producing carbonate and bicarbonate ions (Erşan et al. 2015). This process is used by microorganisms to oxidize organic compounds for energy and cell growth under anaerobic or low-oxygen conditions by reducing nitrate to nitrogen gas, and thus it is expected to be relevant in environments where nitrate and organic carbon are present, and oxygen is limited (Erşan et al. 2015; Singh et al. 2015). A number of bacteria are capable of reducing nitrate such as those belonging to several species of the genera *Alcaligenes*, *Bacillus*, *Denitrobacillus*, *Thiobacillus*, *Pseudomonas*, *Spirillum*, *Micrococcus,* and *Achromobacter* (Erşan et al. 2015; Singh et al. 2015). Similar to ureolysis, the ammonification of amino acids through microbial metabolism is another process that may lead to carbonate precipitation by producing carbonate and ammonia, and increasing the pH and carbonate concentration around the cells (Zhu and Dittrich 2016). This mechanism has been well documented in Myxobacteria that can utilize amino acids as their sole nitrogen, carbon (and energy) sources (González-Muñoz et al. 2010).

In this study, we conducted a preliminary characterization of heterotrophic bacteria living on underwater leafy concretion surfaces of Grotta Giusti. Then we characterized in more detail a *B. licheniformis* strain because this microorganism was largely predominant over the other species on a low-nutrient medium that was used for screening, and demonstrated strong capability to promote calcite mineralization *in vitro* and to produce antibiotic under same conditions that promoted calcite precipitation. The characteristics of this microorganism led us to envisage plausible mechanisms of microbial adaptation and competition in an environment that is characterized by high calcium levels, and to postulate a possible involvement of dissimilatory nitrate reduction to ammonia, a metabolic process that has been recently characterized in *B. licheniformis* (Sun et al. 2016), in calcite biomineralization.

Materials and methods

Sampling procedures and characteristics of the sampling site

The Grotta Giusti (43°52′00″N 10°49′57.6″E) is located in the territory of Monsummano terme (Tuscany, Italy). Total cave length is 420 m and its deepest explored point is 42 m below mean sea level. Its entrance is 59 m above mean sea level. The cave is divided into four distinct zones

COLOR Online / B&W in Print

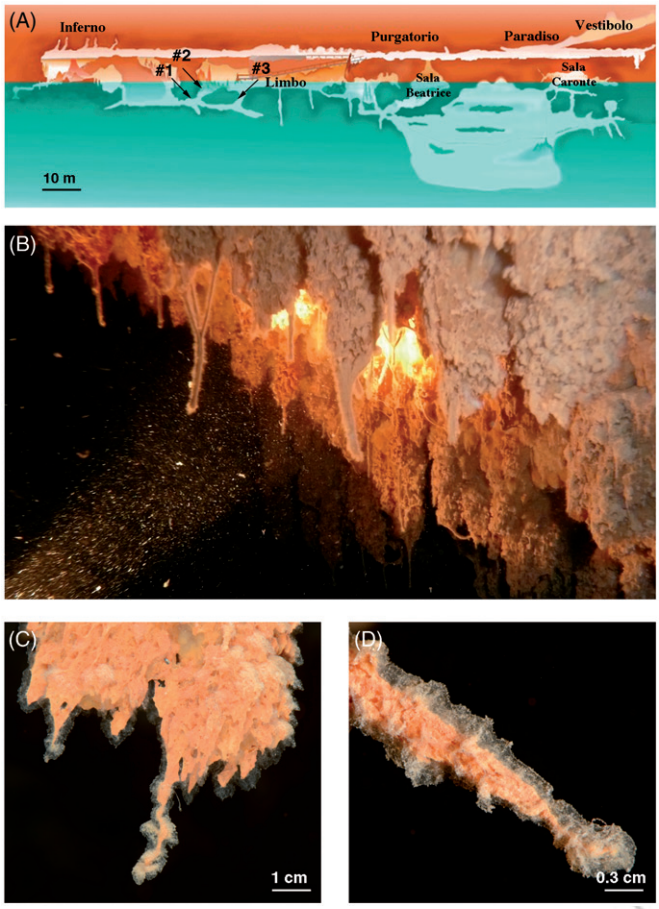

Figure 1. Map of Grotta Giusti and pictures of underwater speleothems. (A) Map of Grotta Giusti with locations of six distinct zones ("Vestibolo", "Paradiso", "Purgatorio", "Inferno", "Sala Beatrice", and "Sala Caronte"). Arrows indicate the three sampling sites (#1, #2, #3). (B) Picture of the cave environment where samples were collected. (C, D) Underwater speleothems from which samples were collected for microbiological analysis.

("Vestibolo", "Paradiso", "Purgatorio" and "Inferno" in Figure 1(A)) that are characterized by a gradual temperature increase from 27.0 to 34.2 °C. The bottom of the cave is characterized by thermal water that flows at the speed of about 1 m/min in east to west direction to reach a small lake ("Limbo" in Figure 1(A)). Here, the temperature always remains at 36 °C with 98% of relative humidity. The composition of the air of the cave is characterized by a high concentration of CO_2 that reaches values about three-times higher than outdoor air (Cigna and Forti 1986). The high groundwater temperature is due to a high geothermal gradient coming from the considerable depth of the water table in faults that intercept deep aquifers (2000–2500 m deep) in Mesozoic carbonate rocks (Bencini et al. 1977; Duchi et al. 1998). Groundwater recharge is of meteoric origin as shown by δ^2H and $\delta^{18}O$ isotopic analyses (Piccini 2000).

In this study, samples of underwater concretions were collected in Autumn 2016 by scuba diving at a depth of 10 m below mean sea level, stored at 4 °C and processed within three days. Sampling was carried out using a splitting chisel according to the best practices with reference to procedures aimed at limiting both sample contaminations by exogenous microorganisms, and the impact on cave environment. Regarding the first point, scuba diving gear was cleaned with mild detergent, and sterile chisel and sample containers were used. Regarding the latter point, we limited the number of samples to three. Examined concretions were about 1 cm in width, length and thickness. The sites where samples were collected are indicated (Figure 1(A), arrows). Although the Monsummanno spa complex is visited annually by thousands of tourists, access to the sampling sites is not allowed to visitors. The temperature at the sites was about 34 °C.

Water chemistry

Table S1 summarizes the data of the chemical and physical analysis of the Limbo water carried out by Agenzia Regionale per la Protezione Ambientale della Toscana (ARPAT) – Regione Toscana over the period 2007–2011 (Mantelli et al. 2014). The urea concentration was determined in this study by QuantiChromTM Urea Assay Kit (BioAssay Systems). Concentration was below the detection limit of the test (0.08 mg/l). Information about possible mineral phases and their Saturation Indices in Limbo water were obtained by using WEB-PHREEQ free available at the Department of Geosciences of North Dakota State University (https://www.ndsu.edu/webphreeq/), a WWW implementation of the aqueous geochemical modeling program PHREEQC (Parkhurst 1995). For geochemical modeling WEB-PHREEQ was run with default options ("simple speciation"; "a single solution") by using the PHREEQC database. pH was used in the modeling by "floating" option. Data reported in Table S1 were used as input. "Full output" was selected as option output. Saturation index (SI) is defined as SI = log (IAP) – log (KT), where IAP is the ion activity product, and KT the solubility constant of the mineral phase.

Microbiological media and cultivation equipment

The composition (per liter) of the microbiological media used in this study is here reported. Medium B (Starkey 1938): 0.5 g K_2HPO_4; 1 g NH_4Cl; 1 g Na_2SO_4; 0.1 g $CaCl_2$ $2H_2O$; 2 g $MgSO_4$ $7H_2O$; 5 g sodium lactate (70% solution); 0.5 g $FeSO_4$ $(NH_4)_2SO_4$ $6H_2O$ (pH 7.4 at 25 °C). When required, 15 g agar per liter was added. B4 medium (Boquet et al. 1973): 4 g yeast extract, 5 g dextrose, 2.5 g $Ca(CH_3COO)_2$ (pH 6.3 at 25 °C). B4-nitrate medium was prepared by supplementing B4 with 0.2 g $NaNO_3$ (per liter). When required, 15 g agar per liter was added. Christensen's urea agar (Christensen 1946): 1 g peptone, 1 g dextrose, 5 g NaCl, 1.2 g Na_2HPO_4, 0.8 g KH_2PO_4, 20 g urea, 12 mg phenol red, 15 g agar (pH 6.8 at 25 °C). This medium was prepared by mixing the indicated ingredients. The phenol red was used as a pH indicator during growth. All reagents were provided by Sigma-Aldrich except for agar (BD™ Difco™ Agar), yeast extract (BD™ Difco™ Yeast Extract), and peptone (Oxoid™ Peptone Bacteriological), which were provided by ThermoFisher Scientific.

Microbiological media were routinely sterilized by autoclaving at 121 °C for 30 min (Autoclave Alfa 10 Plus). Heat-labile media supplements were filtered through 0.45 µm

cellulose acetate filters (VWR International). The pH of all media was not adjusted. All microbiological manipulations were carried out under laminar airflow class II biological safety cabinet (Jouan MSC 12 class II A2 BioSafety Cabinet by Thermo Fisher Scientific). Agarized media were prepared in 90 or 140 mm petri dishes. Thermostatic incubators (Model B 28 provided by Binder; KIC PVX 60M LIGHT TOUCH R134A provided by Mondial Group Srl) were used for cultivation of bacteria on agarized media. Uninoculated media were always included as a negative control. For low-oxygen (capnophilic) growth conditions candle jar was introduced into the thermostatic incubator. Broth cultures were prepared in 15 ml tubes (43766 provided by Corning), 50 ml tubes (430828 provided by Corning), 500 ml or 100 ml Erlenmeyer flasks. Thermostatic orbital shaker-incubator (Innova 43 Large-Capacity Incubator Shaker) was used for broth cultures under aerobic conditions. For low-oxygen growth broth cultures were incubated in Erlenmeyer flasks inside candle jars positioned on the thermostatic orbital shaker-incubator.

For geochemical modeling of B4 and B4 media WEB-PHREEQ was run with default options ("simple speciation"; "a single solution") by using the PHREEQC database. pH was used in the modeling by "floating" option. Modeling was carried out by using as input the elemental composition of media (without yeast extract, dextrose and acetate), and log pCO_2 and log pO_2 default values −3.46 and −0.678 Bar, respectively, for aerobic conditions, and −1.517 and −0.818 Bar, respectively, for low-oxygen conditions. "Full output" was selected as option output.

Isolation and characterization of bacteria from underwater concretions

From each of the three speleothem samples (leafy concretions), three samples of about 100 mg were taken, placed in 1 ml of sterile physiological solution (0.9% NaCl), fragmented by scalpel, and re-suspended thoroughly by vortexing for 4–5 min at room temperature to detach microorganisms residing at the water-speleothem interface or living in the biofilm. To remove debris, samples were centrifuged at 2000*g* for 1 min. Then, 1:10 serial dilutions of the supernatant were transferred onto the surface of Medium B agar, plated in quadruplicate and incubated under aerobic (two plates) or low-oxygen (two plates) conditions for 24–72 h at 30 °C. After this incubation time, a number of colonies with distinct morphology were picked up from each agar plate media (only plates with colony numbers ranging from 50 to 200 were used), streaked onto fresh plates, and incubated for 24–72 h at 30 °C for isolation of pure cultures. Colonies were routinely streaked at least twice to obtain pure cultures. Pure cultures were checked by microscopy, and stored either in above mentioned agar slants or in broth plus 20% (v/v) glycerol at −80 °C.

Colony morphology was examined by using Nikon SMZ 800 N stereomicroscope. Bacterial isolates were biochemically characterized by using the API50CH (Logan and Berkeley 1984) and/or API20NE (Geiss et al. 1985) strip tests provided by bioMérieux, Inc. For each isolate three colonies were examined.

Analysis of antibiotic production by microbiological assay

Antibiotic production by *B. licheniformis* GG-2, which was isolated from underwater speleothems of Grotta Giusti, was evaluated by microbiological assay using agar diffusion methods (Balouiri et al. 2016). The agar plug diffusion method (Balouiri et al. 2016) was used to detect antibiotic production when the strain was cultivated on solid media. To this purpose, after the desired cultivation time, 1.6 cm (diameter) agar discs (with the bacterial layer on the surface) were removed and placed into Petri dishes filled with 5 ml of soft nutrient agar enriched with *Micrococcus luteus* (0.3 $O.D._{600\,nm}$/ml) as a tester microorganism. Plates were then incubated overnight at 37 °C. This temperature is standard for *M. luteus* growth in microbiology assays (Europarat. European Department for the Quality of Medicines 2016).

DNA extraction

Bacterial isolates were grown in 20 ml of Medium B broth with rotary shaking to late logarithmic phase. After centrifugation at 2000*g* for 20 min, pellets were re-suspended in 500 µl of SET buffer (75 mM NaCl, 25 mM EDTA, 20 mM Tris–HCl, pH 7.5). Lysozyme was added at final concentration of 1 mg/ml (w/v), and samples were incubated at 37 °C for 1 h. Then, sodium dodecyl sulfate (SDS) and proteinase K were added, respectively, at final concentration of 1% (v/v) and 0.5 mg/ml (w/v), and samples were incubated at 55 °C for 2 h in a water bath and periodically stirred. Total nucleic acids were extracted by phenol:chloroform:isoamylic alcohol (25:24:1 [v/v/v]) method as described (Sambrook and Russell 2001), and Rnase A (15 µg/ml final concentration for 30 min at 37 °C) was used to remove contaminant RNA. After the extraction, high-molecular weight DNA was precipitated by adding 1/10 volume of 3M sodium acetate and 2.5 volumes of cold 100% ethanol (Sambrook and Russell 2001), recovered by centrifugation, and re-suspended in water at about 1 mg/ml final concentration after quantification by agarose gel electophoresis. The DNA was then used as template in polymerase chain reactions (PCRs) to amplify 16S rRNA-encoding genes or to perform BOX-PCR genomic fingerprinting (Pizzolante et al. 2017; Versalovic et al. 1994)

BOX-PCR genomic fingerprinting

BOX-PCR genomic fingerprinting was done on all isolates as previously described (Pizzolante et al. 2017; Versalovic et al. 1994) using the BOXA1-R primer (5′-CTACGGCAAG GCGACGCTGACG-3′). PCR products were separated on a 1% (w/v) agarose gel in 1 × TBE buffer (Sambrook and Russell 2001). This analysis led us to identify 14 different genomic patterns.

16S rRNA gene sequencing

The bacterial isolates were initially characterized by partial 16S rRNA-encoding gene sequencing by using the bacteria-specific primers Com1-F and Com2-R (Lane et al. 1985). These primers target a 409-nucleotide-long central region of 16S rRNA gene (from nucleotide 519 to nucleotide 926 in the *Escherichia coli* 16S rRNA gene).

To determine almost the entire 16S rRNA gene sequence (from nucleotide 20 to nucleotide 1488 of the corresponding *E. coli* sequence), the bacterial DNA was amplified and sequenced by using the primer pairs 16SE20-42-F/16SEB683-R (corresponding to *E. coli* positions 20–683) (Di Giacomo et al. 2007; Vigliotta et al. 2007), Com1-F/Com2-R (Lane et al. 1985), and 16SEB785-F/16SEB1488-R (corresponding to *E. coli* positions 785 to 1488) (Di Giacomo et al. 2007; Vigliotta et al. 2007). These primer pairs amplified concatenated (and partially overlapping) DNA regions.

PCR products were separated by agarose gel in 1 × TAE buffer (40 mM Tris–acetate, 1 mM EDTA, pH 8.0), recovered by using the Qiaex II gel extraction kit (Qiagen), and sequenced by using the same primers pair utilized for the respective amplifications. DNA sequencing of PCR products was carried as a service (value read tube sequencing service) by Eurofins Genomics (Germany) by using the cycle sequencing technology (dideoxy chain termination/cycle sequencing) on ABI 3730XL sequencing machines. The sequences of bacterial isolates were compared with those of their closely related reference strains present in EzTaxon-e server (now EzBioCloud) (Kim et al. 2012) accessible over the internet at http: https://www.ezbiocloud.net/.

PCR-SSCP genetic profiling

Total DNA was extracted from a mix of the three speleothem samples (leafy concretions). To this purpose, about 1 g of each of the three speleothem samples (total, about 3 g) were collected together into a 13 ml sterile centrifuge tube. Then 4.5 ml of SET buffer was added, and samples were fragmented by vortexing for 10 min. Lysozyme was added at final concentration of 1 mg/ml (w/v), and samples were incubated at 37 °C for 1 h. Then, sodium dodecyl sulfate (SDS) and proteinase K were added, respectively, at final concentration of 1% (v/v) and 0.5 mg/ml (w/v), and samples were incubated at 55 °C for 2 h in a water bath and periodically stirred. Total nucleic acids were extracted by phenol:-chloroform:isoamylic alcohol (25:24:1 [v/v/v]) method as described (Sambrook and Russell 2001), and Rnase A (final concentration 15 µg/ml) was used to remove contaminant RNA. After the extraction, high-molecular weight DNA was precipitated by adding 1/10 volume of 3 M sodium acetate and 2.5 volumes of cold 100% ethanol (Sambrook and Russell 2001), recovered by centrifugation, and re-suspended in water at about 0.5 mg/ml final concentration after quantification by agarose gel electophoresis. Approximately 25 µg of DNA were extracted from the three pooled samples by this procedure.

~~Generation of~~ PCR-SSC genetic profiles were obtained as described (Di Giacomo et al. 2007) with minor modifications. Com1-F and Com2-R were used to amplify 16S rRNA genes from total DNA of the speleothem microbial community. Each PCR was performed with Ampli Taq DNA polymerase (Applied Biosystems) and a 1-min elongation time. PCR products were separated by electrophoresis in a 1% agarose gel in 1× TAE buffer, and purified by using a Qiaex II DNA purification kit (Quiagen). About 9 µl of purified PCR sample was denatured by adding 12 µl of formamide loading buffer (80% [wt/vol] deionized formamide, 10 mM EDTA [pH 8], 1 mg/ml xylene cyanol FF, 1 mg/ml bromophenol blue) at 95 °C for 5 min and then resolved by 7% polyacrylamide (49:1) gel electrophoresis in 0.8× Tris-borate-EDTA (TBE) buffer at 25 mA and 4 °C. Gels were silver stained according to standard procedures. Selected bands identified in SSCP polyacrylamide gels were excised with a razor blade. Blocks of gel were transferred in 50 µl of sterile water, and the DNA was allowed to diffuse overnight at 4 °C. The eluted DNA was reamplified with the same primers and PCR conditions described for PCR-SSCP analysis, and subject to DNA sequencing. DNA sequencing of PCR products was carried as a service (value read tube sequencing service) by Eurofins Genomics (Germany) by using the cycle sequencing technology on ABI 3730XL sequencing machines.

Calcium carbonate biomineralization *in vitro*

To produce calcite microcrystals, bacteria (from frozen glycerol stocks) were streaked on Medium B agar and incubated for 24–72 h at 30 °C. Then three colonies from each bacterial isolate (14 bacterial isolates were totally examined) were streaked in quadruplicate on B4 agar, B4-nitrate or Christensen's urea agar, and incubated for 48–168 h at 30 °C under either aerobic or low-oxygen conditions. Cultures were examined with a stereomicroscope each day. Microcrystals were visible on colony surface after 48–168 h of incubation depending on the different isolates. The microcrystals were collected by boiling (for 20 min) and filtering (Millipore filter 0.45 µm) a small piece of agar medium containing a colony as described (Tiano et al. 1999). Microcrystals were then analyzed by X-ray diffraction (XRD) and Raman microprobe spectroscopy.

To analyze microcrystal production in broth cultures, bacteria were cultivated in shake flasks at 30 °C with B4 broth or B4-nitrate broth under aerobic or low-oxygen conditions. Uninoculated flasks were used as negative controls. Starting from bacteria pre-inoculated and grown over night in 500 ml-shake flasks at 30 °C with 100 ml of B4 broth, four sets of ten 100 ml-flasks (corresponding to the time points: 0, 4, 8, 24, 28, 32, 48, 52, 56, 72 h) with 20 ml of B4 broth were prepared. Two sets of flasks were incubated under aerobic conditions, and two sets were incubated under low-oxygen conditions. The same procedure was used to prepare four additional sets of flasks with 20 ml of B4-nitrate. The duplicated cultures were harvested at the different time points to determine growth, pH, ammonium, nitrite and nitrate concentration. Total precipitated calcium carbonate was determined at 72 h. Growth was measured by colony forming unit method by plating sample dilutions on LB

agar. Ammonium, nitrite and nitrate levels were measured during the time course by using spectrophotometric method. To this purpose, samples were centrifuged at 10,000*g* for 5 min to remove bacteria and calcium carbonate. Before the assays, the samples were diluted 1:4 in sterile water. Ammonium concentration was determined by using the Nessler's reagent; nitrite and nitrate concentrations were determined with the Griess reaction (Griess 1879) and the Griess reaction with cadmium (Cataldo et al. 1975; Navarro-Gonzalvez et al. 1998), respectively. Hydrocheck Colortest Kits (Reasol S.r.L.) were used for ammonium, nitrite and nitrate assays following the manual's instruction. Calibration curves were generated by using B4 broth containing different ammonium chloride, sodium nitrate and sodium nitrite concentrations. Precipitated calcium carbonate was measured as described (Wei et al. 2015). In particular, after 72 h of growth samples were centrifuged at 10,000*g* for 5 min. Then, the pellets (containing bacteria and calcium carbonate) were re-suspended in 2 ml TE buffer (10 mM Tris–Cl, 1 mM EDTA, pH 8.5), and lysozyme was added at a final concentration of 1 mg/ml. Samples were incubated at 37 °C for 1 h with shaking to digest bacterial cell wall. After digestion, cell debris and precipitated calcium carbonate were separated by centrifugation at 10,000*g* for 5 min. Pellets were washed with distilled water, air dried at 37 °C for 24 h, and weighted to estimate the amounts of calcium carbonate precipitated by the different bacteria under the different growth conditions. Precipitates were also analyzed by XRD diffraction, Raman microprobe spectroscopy, and scanning electron microscopy coupled with energy dispersive X-ray spectroscopy (SEM-EDX). For these experiments, precipitates were collected by filtration through a Millipore filter (0.45 µm) as described (Barabesi et al. 2007). Filters were dried at 60 °C overnight.

X-ray diffraction. XRD was used to identify the mineralogy of the crystalline solid produced by bacteria. The samples were pounded to a fine powder in an agate mortar under sterile conditions, homogenized and subsequently analyzed by using a diffractometer Rigaku model Mini Flex with Cu-Kα radiation ($\lambda = 0.154$ nm). The measurements were carried out with 30 kV of accelerating voltage, 15 mA of current, scan angle in 2Θ from 5° to 80°, with step size of 0.01° and scan speed of $0.05°{\cdot}s^{-1}$. Three scans for each measurement were performed. XRD patterns were manually compared with standard calcite and aragonite XRD patterns from the database www.rruff.info.

Raman microprobe spectroscopy

The samples were pounded to a fine powder in an agate mortar under sterile conditions, homogenized and subsequently analyzed. Raman analyses were achieved by using a spectrometer Renishaw model Invia (spectral resolution: $0.5\ cm^{-1}$; Raman spectral range: 100–3000 cm^{-1}) with an argon-ion laser ($\lambda = 514.5$ nm) and a LEICA metallographic microscope. The laser beam was focused on the sample with 15 mW of excitation power. The spectra were acquired for 20 accumulations by 100 s and repeated on five different points. Then an average of Raman spectra was obtained. The spectra were obtained without manipulation and/or baseline correction. *Scanning electron microscopy coupled with energy dispersive X-ray spectroscopy* A scanning electron microscope Jeol JSM 5410-LV coupled to an Oxford Link ISIS 300 Series energy-dispersive spectrometer having a Si(Li) windowless detector was used to perform EDX microanalysis of micro-crystals with the allowed resolution of 156 eV. SEM observations were performed by placing the samples on carbon tape without further handling, but operating in the low-vacuum mode to avoid contamination and sample damage. SEM images have been recorded by backscattered electrons (BSE) with an accelerating voltage of 20 kV and a beam current of 80 µA. Atomic composition (% wt) was expressed as average value and standard deviation of ten measurements for each sample.

GenBank accession numbers

The 16S rRNA gene sequences of the 14 bacterial isolates were deposited at GenBank with the following accession numbers: *B. licheniformis* GG-2 (MF045147), *B. licheniformis* GG-CJ (MF045133), *B. licheniformis* GG-8F (MF045134), *B. mycoides* GG-2RB (MF045135), *Bacillus* sp. GG-5R (MF045136), *Paenibacillus* sp. GG-A (MF045137), *Pseudomonas* sp. GG-4AR (MF045138), *Pseudomonas* sp. GG-8AR (MF045139), *Pseudomonas aeruginosa* GG-1R (MF045140), *P. aeruginosa* GG-4R (MF045141), *P. aeruginosa* GG-7R (MF045142), *P. aeruginosa* GG-2AR (MF045143), *Vogesella indigofera* 7AR (MF045144), *Sphingomonas* sp. 2RM (MF045145).

Results

Culture-based characterization of microorganisms from speleothem samples

Figure 1(B) illustrates the cave environment where samples were collected, which is characterized by vertical roof concretions (leafy concretions) that are covered by matrix (biofilm) embedding white calcium carbonate precipitates. Details of the underwater speleothems from which samples were collected for microbiological, compositional and crystallographic analyses are shown in Figure 1(C, D). The concretion from sampling site #1 (Figure 1(A)) was mainly composed of calcite as demonstrated by XRD (Figure 2) and Raman microprobe spectroscopy (Figure 3). No aragonite could be detected. The same results were obtained with concretions from the sampling sites #2 and #3 (data not shown). Table S1 summarizes the data of the chemical and physical analysis of the Limbo water over the period 2007–2011 (Mantelli et al. 2014). Water geochemical modeling by using WEB-PHREEQ indicated dolomite, calcite and aragonite as possible mineral phases with respectively decreasing SI (i.e., dolomite SI > calcite SI > aragonite SI) (Table S2).

Bacteria from three subaqueous concretions collected from the sampling sites shown in Figure 1(A) were then characterized by culture-dependent methods. To this purpose, sample dilutions were plated on Medium B agar for isolation of microorganisms. Medium B is a chemically

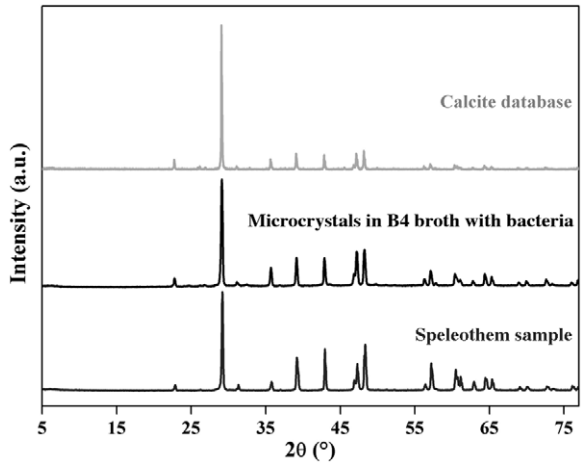

Figure 2. XRD pattern of a standard calcite, of the microcrystals in B4 broth with bacteria grown under aerobic conditions, and of the original concretion from sampling site #1 of the hydrothermal karst cave.

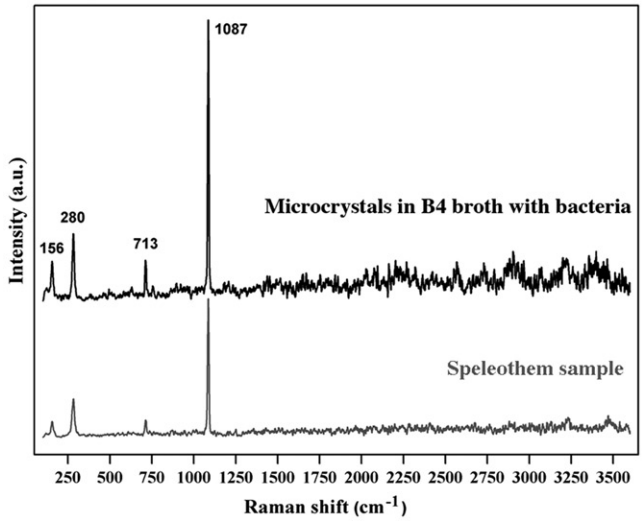

Figure 3. Comparison between the Raman spectrum of the microcrystals in B4 broth with bacteria grown under aerobic conditions, and of the original concretion from hydrothermal karst cave.

defined medium that contains lactate as carbon source, and allows growth of heterotrophic bacteria (Starkey 1938). Bacterial colonies were detected after cultivation at 28 °C for 24–72 h under low-oxygen conditions. Mean microbial titers on speleothem surface were about 2×10^5 colony-forming units per cm^2 for all three speleothem samples. A total of 50 colonies belonging to distinct morphotypes were then isolated and examined. The 50 bacterial isolates from Medium B were subject to DNA extraction and preliminary grouped by using the BOX-PCR fingerprinting technique, based on the use of a single BOX-A1R primer which targets the repetitive BOX regions scattered in the genome of bacteria and results in strain-specific fingerprinting (Versalovic et al. 1994). This technique has been successfully used to analyze the microdiversity of bacterial communities (Pizzolante et al. 2017). The fingerprints were composed of 4–12 major bands with sizes ranging from about 250 to 3000 bp. The results of these analyses demonstrated the presence of 14 different fingerprint patterns (data not shown).

The bacterial isolates (one for each genomic pattern) were then tentatively identified by partial 16S rRNA-encoding gene sequencing (Table 1). The bacterial isolates GG-2, GG-CJ1 and GG-8F could be assigned to group VI *Bacillaceae* species (including the species *Bacillus insolitus*, *B. licheniformis*, *Bacillus amyloliquefaciens*, *Bacillus atrophaeus*, *Bacillus mojavensis*, *B. subtilis*, *Bacillus fusiformis*, and *Bacillus sphaericus*) (Xu and Côté 2003). Morphological and biochemical traits (Table S3) indicated that all these isolates belong to the species *B. licheniformis*. The isolate GG-5R shared 100% identity with type strains of the species *Bacillus indicus* and *Bacillus idriensis*, while the isolate GG-A (that failed to grow on API50CH strips) shared the same percent identity with the species *Paenibacillus humicus* and *Paenibacillus pasadenensis* at the level of 16S rRNA gene sequence. The isolate GG-2RB was related to group X *Bacillaceae* species (including the species *Bacillus cereus*, *Bacillus mycoides*, *Bacillus thuringiensis*, *Bacillus anthracis* and *Bacillus lentus*) (Xu and Côté 2003). Morphological and biochemical traits (Table S3) indicated that this isolate belongs to the species *Bacillus mycoides*. Among Gram-negatives, the isolates GG-1R, GG-4R, GG-7R and GG-2AR could be assigned to the species *Pseudomonas aeruginosa* consistently with biochemical data (Table S4), while the isolates GG-4AR and GG-8AR were assigned to the species *Pseudomonas balearica* and *Pseudomonas sihuiensis*, respectively. Slow growing GG-7AR (whose small-sized, blue-pigmented colonies appeared after 72 h incubation in Medium B) was identified as *Vogesella indigofera* (that failed to grow on API20NH strips), while the isolate GG-2RM shared 100% identity with type strains of the species *Sphingomonas panni* $C52^T$ and *Sphingomonas hankookensis* $ODN7^T$.

Characterization of calcite-mineralizing *Bacillus licheniformis* GG-2

We examined the ability of the isolated bacteria to grow and form microcrystals in the presence of high levels of Ca^{2+}. On Ca^{2+}-rich B4 agar all *Bacillus* spp. isolates GG-2, GG-CJ1, GG-8F and GG-2RB, *Paenibacillus* sp. GG-A and *Pseudomonas* sp. GG-1R, GG-4R, GG-7R, GG-2AR and GG-8AR were able to grow and exhibited abundant production of microcrystals after 48 h as revealed by stereomicroscope observation (Figure 4(A, B) and Table 1), while *Pseudomonas* sp. GG-4AR and *Vogesella* sp. GG-7AR were not able to grow. Microcrystals were never observed in negative controls (i.e., B4 agar without bacteria).

Then we focused our attention to *Bacillus* sp. GG-2 because under the cultivation conditions used in our screening it appeared to be the largely prevalent microorganism based on BOX-PCR profile (about 60% of total isolates), and because it exhibited abundant production of microcrystals on B4 agar. Sequencing of almost the entire 16S rRNA-encoding gene (from nucleotide 20 to nucleotide 1488 of the corresponding *E. coli* sequence) confirmed that this isolate belongs to the species *B. licheniformis* within the group VI of *Bacillaceae* species, which includes other species capable of forming calcite under *in vitro* conditions in the presence

Table 1. Identity of bacterial isolates from submerged speleothems.

Isolate #	Closest reference species and strain in EzBioCloud 16S rRNA databank	Similarity percentage[a]	Biochemical identification by API tests[b]	API test identification confidence percentage	Growth on B4 agar and production of calcite crystals[c]
Bacillus sp. GG-2	*Bacillus amyloliquefaciens* subsp. amyloliquefaciens DSM 7^T *Bacillus*	100	*Bacillus licheniformis*	80.0	++
Bacillus sp. GG-CJ		100	*Bacillus licheniformis*	98.3	++
Bacillus sp. GG-8F	*atrophaeus* JCM 9070^T *Bacillus methylotrophicus* KACC 13105^T *Bacillus siamensis KCTC 13613(T) Bacillus subtilis* subsp. inaquosorum KCTC 13429^T *Bacillus subtilis* subsp. spizizenii NRRL B-23049^T *Bacillus subtilis* subsp. subtilis NCIB 3610^T *Bacillus tequilensis* KCTC 13622^T	100	*Bacillus licheniformis*	78.9	++
Bacillus sp. GG-2RB	*Bacillus cereus* NBRC 15305^T *Bacillus mycoides* DSM 2048^T *Bacillus thuringiensis* WS2617^T	98.10	*Bacillus mycoides*	78.9	++
Bacillus sp. GG-5R	*Bacillus indicus* Sd/3^T *Bacillus idriensis* SMC 4352-2^T	100	n.d.	n.d.	–
Paenibacillus sp. GG-A	*Paenibacillus humicus* PC-147^T *Paenibacillus pasadenensis* SAFN-007^T	100	n.d.	n.d.	+
Pseudomonas sp. GG-4AR	*Pseudomonas balearica* DSM 6083^T	96.72	n.d.	n.d.	+
Pseudomonas sp. GG-8AR	*Pseudomonas sihuiensis* WM-2^T	98.87	n.d.	n.d.	+
Pseudomonas sp. GG-1R	*Pseudomonas aeruginosa* JCM 5962^T	99.75	*Pseudomonas aeruginosa*	99.0	+
Pseudomonas sp. GG-4R	*Pseudomonas aeruginosa* JCM 5962^T	99.75	*Pseudomonas aeruginosa*	99.0	+
Pseudomonas sp. GG-7R	*Pseudomonas aeruginosa* JCM 5962^T	99.75	*Pseudomonas aeruginosa*	99.6	+
Pseudomonas sp. GG-2AR	*Pseudomonas aeruginosa* JCM 5962^T	99.75	*Pseudomonas aeruginosa*	99.0	+
Vogesella sp. GG-7AR	*Vogesella indigofera* ATCC 19706^T	99.54	n.d.	n.d.	–
Sphingomonas sp. GG-2RM	*Sphingomonas panni* C52^T *Sphingomonas hankookensis* ODN7^T	100	n.d.	n.d.	–

[a]Similarity percentage as determined by EzBioCloud.
[b]n.d., not determinable.
[c]n.t., not tested.

of high calcium levels (Anbu et al. 2016; Dhami et al. 2013; Dhami et al. 2014). 16S rRNA gene-based PCR-SSCP profiling confirmed the presence of this group of microorganisms in the bacterial community of underwater speleothems (Figure 5). Indeed, bands with the same electrophoretic mobility were visible in amplified DNA from both speleothem sample (a mix of the three original samples was used) (Figure 5, lane 7) and *B. licheniformis* isolates GG-2 (Figure 5, lane 2) and GG-2RM (Figure 5, lane 4). The identity of recovered bands was verified by DNA sequencing.

A notable feature of *B. licheniformis* GG-2 was its ability to form abundant microcrystals resembling the calcite microcrystals by stereomicroscopy also when cultivated on B4-nitrate agar under low-oxygen conditions (Figure S1(E, F)) or on Christensen's urea agar that is not supplemented with calcium salts (Figure 4(C–F)). Microcrystals were never observed in negative controls (i.e., B4-nitrate agar and Christensen's urea agar without bacteria). On Christensen's urea agar low-oxygen conditions considerably stimulate swarming and the Medusa-head type of growth that was characterized by thin and flat colonies with denticulate edges and finger-like projections with abundant microcrystals also at early incubation times (24 h) (Figure S1(A, B)).

Growth (Figure 6(A)), pH (Figure 6(B)) and calcium carbonate precipitation (Figure 6(C)) were then evaluated in B4 and B4-nitrate broths. In the B4-nitrate broth nitrate utilization and production of nitrite and ammonia were also determined. Results showed that the nitrate supplement stimulated (>4-fold) calcium carbonate precipitation (evaluated at 72 h) under low-oxygen condition (Figure 6(C)); in contrast calcium carbonate precipitation was not affected by nitrate supplement when bacteria were cultivated under aerobic conditions. Amounts of precipitated calcium carbonate were similar in B4 and B4-nitrate broths under aerobic conditions, and about 33% higher than in B4-nitrate broth under low-oxygen conditions (Figure 6(C)). Under low-oxygen conditions the nitrate supplement resulted in greater alkalization of the medium during the bacterial growth as compared to the other growth conditions (Figure 6(B)). Results of measurement of nitrate, nitrite and ammonium levels at different time points indicated that nitrate were consumed by bacteria under both aerobic and low-oxygen conditions (Figure 6(D)). However, the bacteria released more ammonium (Figure 6(F)) and less nitrite (Figure 6(E)) when they were grown under low-oxygen compared to when they were cultivated under aerobic conditions. Ammonium concentrations were also determined in B4 under either aerobic or low-oxygen conditions, and were below 5 µM at all time points (data not shown).

Interestingly, the same conditions that promoted calcite precipitation also appeared to stimulate antibiotic production by *B. licheniformis* GG-2 (Figure 7 and data not shown). Results of microbiology assays using *M. luteus* as a tester

COLOR Online / B&W in Print

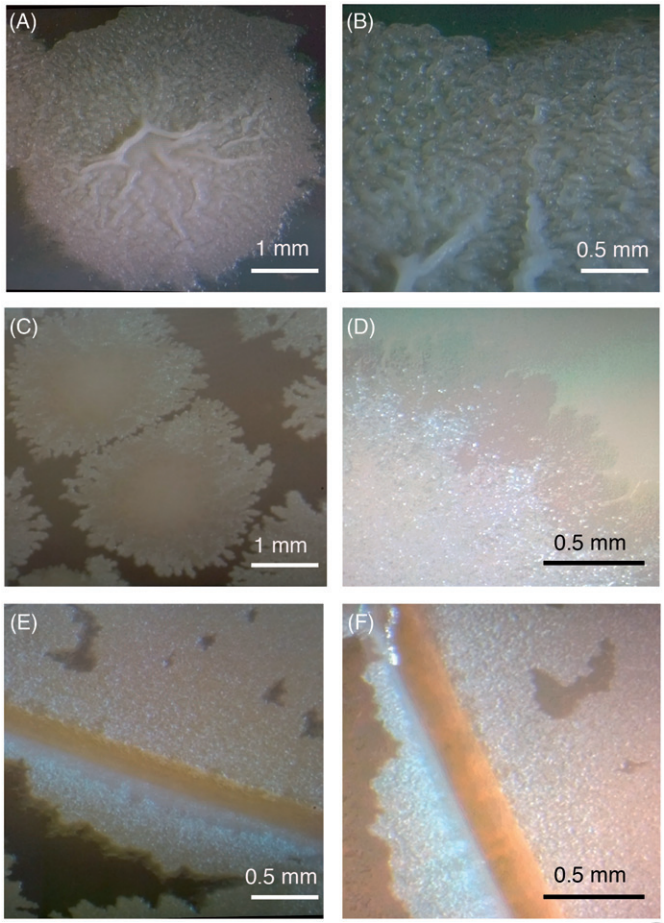

Figure 4. Colony morphology and microcrystals produced by *B. licheniformis* GG-2. (A, B) Colonies formed by bacteria cultivated on B4 agar for 48 h under aerobic conditions. (C, D) Colonies formed by bacteria cultivated on Christensen's urea agar for 48 h under aerobic conditions. (E, F) Details of a colony growing on Christensen's urea agar after 48 and 168 h, respectively.

microorganism demonstrated antibiotic activity in both B4 and B4-nitrate agar, and less pronounced production in Christensen's urea agar, while antibiotic activity could not be detected when urea was not added to Christensen's urea agar.

Characterization of the calcite microcrystals by XRD, Raman microprobe spectroscopy and SEM-EDX

The nature of the microcrystals was then investigated by XRD and Raman microprobe spectroscopy. In Figure 2, *B. licheniformis* GG-2 was cultivated in B4 broth for four weeks at 30 °C in shake flasks under aerobic conditions. Then precipitates that formed in the medium were collected and analyzed as described in the Materials and Methods section. Figure 2 shows the comparison between the XRD spectra of the crystals induced by bacteria, and of the original concretion from hydrothermal karst cave. XRD pattern includes the dominant peak of the calcite (104) at $2\Theta = 29.3°$, as well as other characteristic peaks (012), (110), (113), (202), (018), (116) and (1010), at 22.7°, 35.6°, 39.2°, 42.8°, 47.2°, 48.3° and 57.5°, respectively, as expected from a rhombohedral primitive cell with $a = 0.5038$ nm and $c = 1.7325$ nm (Belcher et al. 1996; Fu et al. 2005; Rahman and Oomori, 2008). The figure also shows the spectrum of pure calcite from the database www.ruff.org. XRD pattern

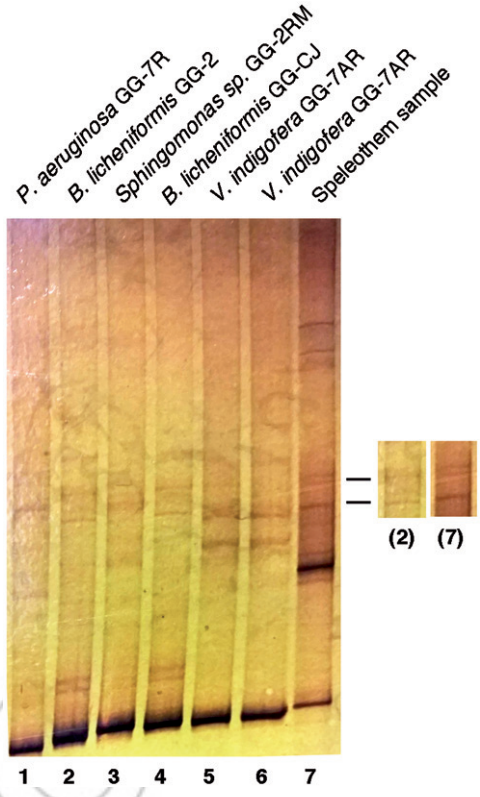

Figure 5. PCR-SSCP genetic profiling of the bacterial community living of underwater speleothems. The profile was generated with the Bacteria-specific primer pair Com1-F/Com2-R. Total DNA was amplified from the indicated bacterial isolates (lanes 1–6) or speleothem samples (lane 7). On the right of the gel details from lanes 2 and 7 are illustrated to indicate the positions of the bands (marked by lines) with the same electrophoretic mobility.

shows that the crystals formed in the presence of bacteria and original concretion from hydrothermal karst cave are both calcite. Similar results were obtained when the *B. licheniformis* GG-2 was cultivated in B4-nitrate broth, B4 agar, B4-nitrate agar, or Christensen's urea agar, and incubated under either aerobic or low-oxygen conditions (data not shown). Noteworthy, Saturation Indices (SIs) indicate that B4 medium and B4-nitrate medium are supersaturated with respect to calcite and aragonite with similar SIs (Table S5). However, only calcite could be detected by XRD.

Raman microprobe spectroscopy (Figure 3) revealed the same crystalline phase as shown by XRD analysis, which is calcite for both the samples (crystals induced by *B. licheniformis* GG-2 in B4 broth under aerobic condition, and of the original concretion). In fact, the analyzed crystals of both samples formed by bacteria and of the original concretion exhibited the characteristic A_{1g} and E_g double degenerates Raman active modes of rhombohedric calcite with the bands at 156, 280, 713 and 1087 cm^{-1} (De La Pierre et al. 2014; Edwards et al. 2005). Similar results were obtained when the *B. licheniformis* GG-2 was cultivated in B4-nitrate broth, B4 agar, B4-nitrate agar, or Christensen's urea agar, and incubated under either aerobic or low-oxygen conditions (data not shown).

Calcite microcystals were also analyzed by SEM-EDX. Figure 8 shows typical images SEM of microcrystals produced by *B. licheniformis* GG-2 under aerobic conditions after growth in either B4 agar (Figure 8(A, B)) or B4 broth

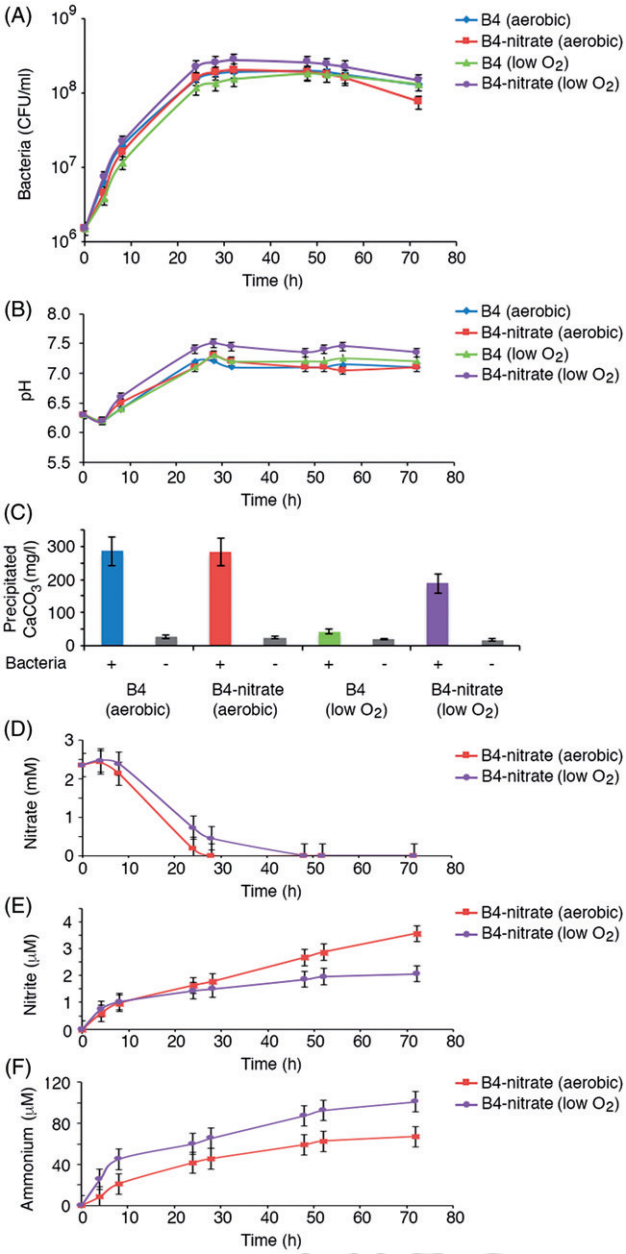

Figure 6. Growth parameters and calcium carbonate precipitation in B4 and B4-nitrate broths. (A, B) Growth curves (A) and pH values (B) of broth cultures in B4 and B4-nitrate media under either aerobic or low-oxygen conditions. (C) Amounts of precipitated calcium carbonate after 72 h of growth in B4 and B4-nitrate media under either aerobic or low-oxygen conditions. Uninoculated media were used as negative controls. (D–F) Nitrate, nitrite and ammonium levels in B4-nitrate broth cultures at different time points under either aerobic or low-oxygen conditions. Values in A–F represent mean ± standard deviations of duplicate samples.

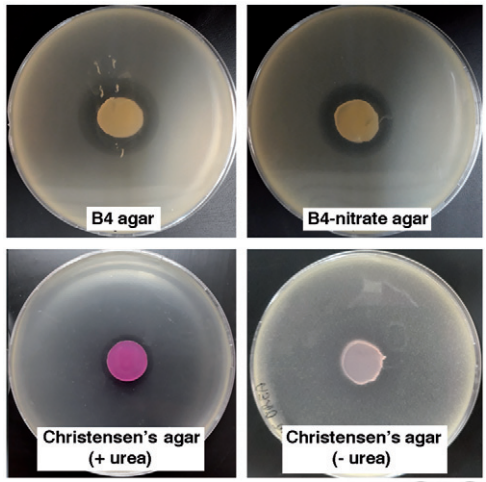

Figure 7. Antibiotic production by *B. licheniformis* GG-2 as detected microbiological assays. *B. licheniformis* GG-2 was cultivated for seven days on B4 agar (aerobic conditions), B4-nitrate agar (low-oxygen conditions), Christensen's urea agar or Christensen's urea agar without urea supplement (aerobic conditions). Then antibiotic production was detected by microbiological assays with *M. luteus* as a tester microorganism.

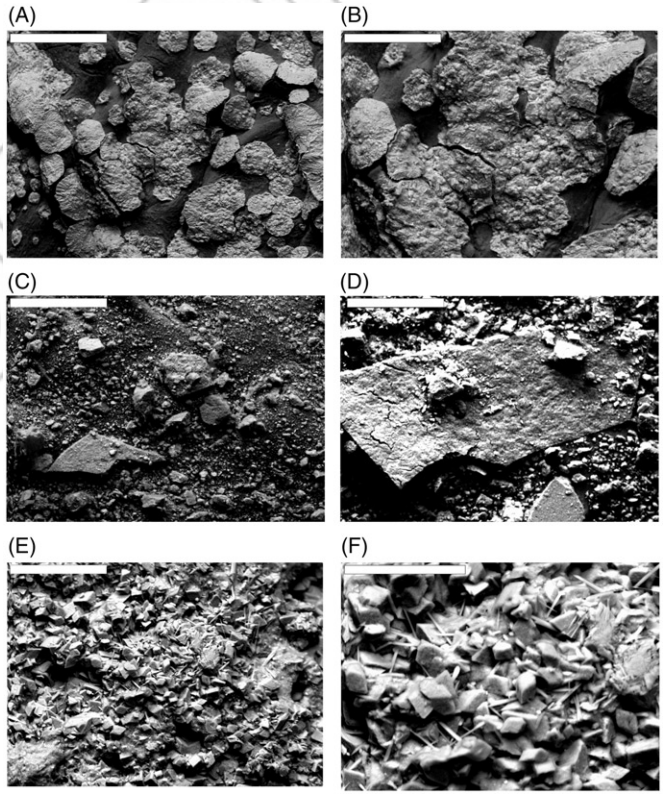

Figure 8. SEM images of calcite microcrystals. Calcite microcrystals produced by *B. licheniformis* GG-2 either in B4 agar (A and B) or B4 broth (C and D) under aerobic conditions, and calcite crystals on the original speleothem samples (E and F) were analyzed. Scale bars: $A = 200\ \mu m$; $B = 100\ \mu m$; $C = 200\ \mu m$; $D = 100\ \mu m$; $E = 100\ \mu m$; $F = 50\ \mu m$.

(Figure 8(C, D)) as compared to calcite crystals on the original speleothem samples (Figure 8(E, F)). EDX data are reported in Table 2. Results demonstrated differences in microtexture between microcrystals produced by *B. licheniformis* GG-2 under the different cultivation conditions. In B4 agar most calcite microcrystals that were recovered from bacterial biofilm formed flat, radial disks (lamellae) (Figure 8(A, B)) of rather homogeneous size. In contrast, calcite microcrystals recovered from B4 broth were highly heterogeneous in size with irregular, polyhedral shape (Figure 8(C, D)). Most microcrystals from the original speleothems were homogeneous in size, and exhibited trigonal or rhombohedral morphology (Figure 8(E, F)). The SEM images also showed needle-like crystals and rare irregularly shaped, radial concretions located under the trigonal and rhombohedral crystal layer (Figure 8(E, F)).

Table 2. Atomic composition (% wt) obtained by SEM-EDX analysisa.

	Speleothem sample	Microcrystals in B4 agar with bacteria	Microcrystals in B4 broth with bacteria
C	3.7 (0.4)	16.9 (0.7)	14.9 (0.5)
O	76.1 (3.5)	67.5 (3.4)	69.4 (3.6)
Ca	15.9 (1.2)	15.3 (0.9)	15.2 (0.7)
Al	1.3 (0.1)	<1	<1
Si	1.9 (0.2)	<1	<1

[a]Table shows the average value and the standard deviation (in brackets) for each element analyzed.

Discussion

Speleothem microorganisms are subject of considerable scientific interest because they provide us with the opportunity of investigating the mechanisms of microbial adaptation to specific environmental conditions. The underwater speleothems of Grotta Giusti represent an underground environment that is characterized by supra-saturated calcium carbonate concentrations. Yet, on speleothem surface we found microbial titers about 2×10^5 colony-forming units per cm^2 using low-nutrient Medium B agar. Group VI *Bacillaceae* and *Pseudomonadaceae* species appeared to be the largely prevalent cultivable microorganisms under the cultivation conditions used in our screening. It is difficult to establish whether the prevalence of these groups of microorganisms may be due to the thousands of tourists that annually visit the Grotta Giusti, and to what extent such a high number of tourists might have an impact on the microbial communities living on the speleothem surfaces.

Bacillaceae licheniformis GG-2, as well as most of the other bacteria that were isolated from the underwater speleothems exhibited growth on Ca^{2+}-rich B4 agar, and abundant production of calcite microcrystals (Figure 4 and Table 1). The exact biological and ecological role of bacteria in calcium carbonate precipitation is still unclear. On one hand, starting from the evidence that almost all bacteria are capable of calcium carbonate precipitation several authors suggest that this process may be considered as a side effect of common metabolic processes including carbon fixation, ureolysis, denitrification, ammonification, sulfate reduction, and methane oxidation (Knorre and Krumbein 2000). These metabolic processes increase the alkalinity of the microenvironment where the microorganisms live thereby promoting calcium carbonate precipitation (Zhu and Dittrich 2016). On the other hand, it has been suggested that calcium carbonate precipitation may play more complex physiological and ecological roles. It may be considered a detoxification response of bacteria to high calcium concentration (Banks et al. 2010) and/or may be functional to the construction of their ecological niche (Chafetz et al. 1991; Folk 1993; Paerl et al. 2001; Vasconcelos et al. 1995; Zavarzin 2002). This latter hypothesis is supported by a strong attitude of cave microorganisms to precipitate calcium carbonate by using not only the above-mentioned metabolic processes but also additional strain-specific mechanisms such as the production of extracellular polymeric substances that trap and concentrate the calcium ions or specific proteins that influence precipitation (Arias and Fernandez 2008; Kawaguchi and Decho 2002; Tourney and Ngwenya 2009). More interestingly, the strain specificity also extends to crystal aggregate morphology (Hammes et al. 2003).

Our findings may be very well placed in this scenario. In bacteria calcium plays key roles in a number of physiologic processes including maintenance of cell structure, motility, cell division, gene expression, and cell differentiation processes such as sporulation, heterocyst formation and fruiting body development (Dominguez 2004; Norris et al. 1996; Smith 1995). However, intracellular calcium concentration must be tightly regulated, and it typically ranges between 100 and 300 nM (Dominguez 2004). Ion channels, primary and secondary transporters, and Ca^{2+}-binding proteins are involved in Ca^{2+} homeostasis (Norris et al. 1996; Paulsen et al. 2000; Waditee et al. 2004). Importantly, calcium carbonate precipitation is particularly beneficial to bacteria in Ca^{2+}-rich cave environments as a mechanism to overcome calcium toxicity (Banks et al. 2010). The adaptive capabilities of *B. licheniformis* in the Ca^{2+}-rich environment of the underwater speleothems may be due to both metabolic and structural features.

Interestingly, the *B. licheniformis* GG-2 isolate was able to form abundant calcite microcrystals also when cultivated on Christensen's urea agar without Ca^{2+} supplement (Figure 4(C–E)) confirming a possible role of urea hydrolysis in calcite biomineralization. Indeed, the hydrolysis of urea presents several advantages over the other calcium carbonate precipitation pathways, as it can be easily controlled, and it has the potential to precipitate high amounts of calcium carbonate within a short period of time. However, the microbial urease activity is greatly influenced by temperature, pH (with an optimal of 7–8.7 except for acid-urease activity), concentration of urea and the end product ammonia, carbon source, and incubation period (Hasan 2000). In this study, we found urea levels in the Limbo water below the detection limits of our assay (0.08 mg/L), although these levels may be subjected to considerable variation over time in aquatic systems (Solomon et al. 2010). Therefore, we could not determine to what extent the urea hydrolysis may be involved in calcite biomineralization.

Dissimilatory nitrate reduction to ammonia is a metabolic process that may be also relevant to calcite biomineralization in the examined underwater environment because of the presence in Limbo water of relatively high levels of nitrate (ranging from 1.7 to 2 mg/l) and reduced oxygen solubility due to the high water temperature (about 34 °C at the sampling site) and salinity. Although *B. licheniformis* has long been considered a denitrifier, both physiological and genomic data have recently demonstrated that under anaerobic/oxygen-limited conditions this bacterium does not denitrify but is capable of fermentative dissimilatory nitrate/nitrite reduction to ammonium (with concomitant production of N_2O) (Sun et al. 2016). The consequent increase in local pH may promote calcium carbonate precipitation. This hypothesis is supported by the abundant production of calcite microcrystals in B4-nitrate agar under low-oxygen conditions (Figure S1(E, F)), and by the evidence that nitrate supplement greatly stimulated calcium carbonate precipitation under low-oxygen condition, while this

stimulatory effect could not be detected when bacteria were cultivated under aerobic conditions (Figure 6).

In addition to metabolic processes, the precipitation of calcium carbonate polymorphs might be influenced by the anionic gamma-glutamyl capsule polymer of *B. licheniformis*, which acts as a scavenger of divalent cations including Ca^{2+} and Mg^{2+} (Njegić-Džakula et al. 2011). These properties have made the calcium carbonate precipitation process by *B. licheniformis* a promising alternative for sealing cement-based materials (Vahabi et al. 2015). Beside, also noteworthy is the gamma-glutamyl capsule-induced formation of amorphous, rust-colored ferrihydrite, a common compound in ochreous speleothems (McLean et al. 1992). Interestingly, the same conditions that promoted calcite precipitation also elicited antibiotic production by *B. licheniformis* GG-2 (Figure 7). The nature of the antibiotic produced under these growth conditions was not defined in this study. However, *B. licheniformis* is a well-known bacitracin A producer (Bernlohr and Novelli 1960; Bernlohr and Novelli 1963), and there is evidence that Ca^{2+} may act as a secondary messenger in elicitation of the bacitracin A synthesis (Reffatti et al. 2013). It would be nice to investigate in the future the nature of this unknown antibiotic to assess its possible role in microbial competition within the biofilm of the underwater speleothems.

To what extent microbial species play an active role in development of calcite deposits on speleothems in cave environment is matter of debate. Analysis of several properties such as mineral texture, crystallinity, grain and crystallite size coupled with water chemistry data may help to evaluate the contribution of physical, chemical and biological processes in calcite mineralization (Pedley 1994; Taylor et al. 2004). Water geochemical modeling of Limbo water indicated dolomite, calcite and aragonite as possible mineral phases with respectively decreasing Saturation Indices (SI) (Table S2), but only the presence of calcite was documented by XRD (Figure 2) and Raman microprobe spectroscopy (Figure 3) in the examined concretions. SEM images revealed some similarity in microtexture between calcite deposits on underwater speleothems (mostly with regular, trigonal or rhombohedral morphology) (Figure 8(E, F)) and calcite microcrystals formed by *B. licheniformis* GG-2 in B4 broth (mostly with irregular, polyhedral shape) (Figure 8(C, D)). In contrast, most calcite microcrystals that were recovered from bacterial biofilm on B4 agar formed flat, radial disks (lamellae) (Figure 8(A, B)) suggesting an active role of bacterial surface structures and extracellular matrix (in addition to bacterial metabolic activities) in the mineralization process on B4 agar. Radial concretions resembling the calcite microcrystals formed in B4 agar were instead rarely observed on the original speleothems. These rare concretions were visible under the abundant trigonal and rhombohedral crystal layer. This finding may suggest a prevalence of abiogenic with respect to biogenic mechanisms in the mineralization process on underwater speleothems. Nevertheless, the bacteria with their metabolic activities might contribute to this process also creating the initial crystal nucleation sites that contribute to the formation of secondary calcium carbonate deposits within the cave providing a further evidence of how microorganisms can remodel our surrounding environment.

Disclosure statement

No potential conflict of interest was reported by the authors.

Funding

The study was carried out using the facilities of "BIOforIU" multidisciplinary infrastructure for the study and valorization of marine and terrestrial biodiversity (project PONa3 00025 funded by Ministero dell'Istruzione, Università e Ricerca).

References

Achal V, Pan X. 2011. Characterization of urease and carbonic anhydrase producing bacteria and their role in calcite precipitation. Curr Microbiol 62:894–902.

Anbu P, Kang CH, Shin YJ, So JS. 2016. Formations of calcium carbonate minerals by bacteria and its multiple applications. Springerplus 5250

Arias JL, Fernandez MS. 2008. Polysaccharides and proteoglycans in calcium carbonate-based biomineralization. Chem Rev 108:4475–4482.

Arp G, Thiel V, Reimer A, Michaelis W, Reitner J. 1999. Biofilm exopolymers control microbialite formation at thermal spring discharging into the alkaline Pyramid Lake, Nevada, USA. Sediment Geol 126(1–4):159–176.

Balouiri M, Sadiki M, Ibnsouda SK. 2016. Methods for in vitro evaluating antimicrobial activity: a review. J Pharm Anal 6:71–79.

Banks ED, Taylor NM, Gulley J, Lubbers BR, Giarrizzo JG, Bullen HA, Hoehler TM, Barton HA. 2010. Bacterial calcium carbonate precipitation in cave environments: a function of calcium homeostasis. Geomicrobiol J 27:444–454.

Barabesi C, Galizzi A, Mastromei G, Rossi M, Tamburini E, Perito B. 2007. *Bacillus subtilis* gene cluster involved in calcium carbonate biomineralization. J Bacteriol 189:228–235.

Baskar S, Baskar R, Mauclaire L, McKenzie JA. 2005. Role of microbial community in stalactite formation, Sahastradhara caves, Dehradun, India. Curr Sci 88:1305–1308.

Baskar S, Baskar R, Mauclaire L, McKenzie JA. 2006. Microbially induced calcite precipitation by culture experiments –possible origin for stalactites in Sahastradhara, Dehradun, India. Curr Sci 90:58–64.

Baskar S, Baskar R, Kaushik A. 2007. Evidences for microbial involvement in the genesis of speleothem carbonates, Borra Caves, Visakhapatnam, India. Curr Sci 92:350–355.

Baskar S, Baskar R, Lee N, Theophilus PK. 2009. Speleothems from Mawsmai and Krem Phyllut caves, Meghalaya, India: some evidences on biogenic activities. Environ Geol 57:1169–1186.

Bazylinski DA, Moskowitz BM. 1997. Microbial biomineralization of magnetic iron minerals: microbiology, magnetism and environment significance. Rev Mineral Geochem 35:181–223.

Belcher AM, Wu XH, Christensen RJ, Hansma PK, Stucky GD, Morse DE. 1996. Control of crystal phase switching and orientation by soluble mollusc-shell proteins. Nature 381:56–58.

Bencini A, Duchi V, Martini M. 1977. Geochemistry of thermal springs of Tuscany (Italy). Chem Geol 19:229–252.

Benzerara K, Miot J, Morin G, Ona-Nguema G, Skouri-Panet F, Ferard C. 2011. Significance, mechanisms and environmental implications of microbial biomineralization. CR Geosci 343:160–167.

Bernlohr RW, Novelli GD. 1960. Some characteristics of bacitracin production by *Bacillus licheniformis*. Arch Biochem Biophys 87:232–238.

Bernlohr RW, Novelli GD. 1963. Biosynthesis and spore formation: the physiological role of antibiotic. Arch Biochem Biophys 10394–104.

Boquet E, Boronat A, Ramos-Cormenzana A. 1973. Production of calcite (calcium carbonate) crystals by soil bacteria is a general phenomenon. Nature 246:527–529.

Botré C, Botré F. 1989. Carbonic anhydrase and urease: an investigation in vitro on the possibility of a synergic action. Biochim Biophys Acta 997(1–2):111–114.
Braissant O, Decho AW, Dupraz C, Glunk C, Przekop KM, Visscher PT. 2007. Exopolymeric substance of sulfate-reducing bacteria: interactions with calcium at alkaline pH and implication for formation of carbonate minerals. Geobiology 5:401–411.
Brennan ST, Lowenstein TK, Horita J. 2004. Seawater chemistry and the advent of biocalcification. Geology 32:473–476.
Broughton PL. 1983a. Environmental implications of competitive growth fabrics in stalactitic carbonate. IJS 13(1/4):31–41.
Broughton PL. 1983b. Lattice deformation and curvature in stalactitic carbonate. IJS 13(1/4):19–30.
Broughton PL. 1983c. Secondary origin of the radial fabric in stalactitic carbonate. IJS 13(1/4):43–66.
Brown JK. 1994. Bootstrap hypothesis tests for evolutionary trees and other dendrograms. Proc Natl Acad Sci U S A 91:12293–12297.
Cacchio P, Contento R, Ercole C, Cappuccio G, Martinez MP, Lepidi A. 2004. Involvement of microorganisms in the formation of carbonate speleothems in the Cervo Cave (l'Aquila-Italy). Geomicrobiol J 21:497–509.
Cataldo DA, Maroon M, Schrader LE, Youngs VL. 1975. Rapid colorimetric determination of nitrate in plant-tissue by nitration of salicylic-acid. Commun Soil Sci Plant Anal 6:71–80.
Chafetz HS, Rush P, Utech NM. 1991. Microenvironmental controls on mineralogy and habitat of CaCO3 precipitates: an example from an active travertine system. Sedimentology 38:107–126.
Christensen WB. 1946. Urea decomposition as a means of differentiating Proteus and paracolon cultures from each other and from Salmonella and Shigella types. J Bacteriol 52:461–466.
Cigna AA, Forti P. 1986. The speleogenetic role of air flow caused by convection. 1st contribution. IJS 15(1/4):41–52.
De La Pierre M, Carteret C, Maschio L, André E, Orlando R, Dovesi R. 2014. The Raman spectrum of $CaCO_3$ polymorphs calcite and aragonite: a combined experimental and computational study. J Chem Phys 140:164509
Dhami NK, Reddy MS, Mukherjee A. 2013. Biomineralization of calcium carbonate polymorphs by the bacterial strains isolated from calcareous sites. J Microbiol Biotechnol 23:707–714.
Dhami NK, Reddy MS, Mukherjee A. 2014. Synergistic role of bacterial urease and carbonic anhydrase in carbonate mineralization. Appl Biochem Biotechnol 172:2552–2561.
Di Giacomo M, Paolino M, Silvestro D, Vigliotta G, Imperi F, Visca P, Alifano P, Parente D. 2007. Microbial community structure and dynamics of dark fire-cured tobacco fermentation. Appl Environ Microbiol 73:825–837.
Dominguez DC. 2004. Calcium signalling in bacteria. Mol Microbiol 54:291–297.
Douglas S, Beveridge TJ. 1998. Mineral formation by bacteria in natural microbial communities. FEMS Microbiol Ecol 26:79–88.
Duchi V, Fazzuoli M, Piccini L, Chiappini L. 1998. Idrogeologia e geochimica del sistema termale di Monsummano. In: Fazzuoli M. (a vcura di). Il Colle di Monsummano Alto: le pietre e le acque, Pisa: Pacini Ed, p. 63–78.
Dupraz C, Visscher PT. 2005. Microbial lithification in marine stromatolites and hypersaline mats. Trends Microbiol 13:429–438.
Edwards HGM, Jorge Villar SE, Jehlicka J, Munshi T. 2005. FT–Raman spectroscopic study of calcium-rich and magnesium-rich carbonate minerals. Spectrochimica Acta Part A 61:2273–2280.
Erşan YC, de Belie N, Boon N. 2015. Microbially induced $CaCO_3$ precipitation through denitrification: an optimization study in minimal nutrient environment. Biochem Eng J 101108–118.
Europarat. European Department for the Quality of Medicines 2016. European Pharmacopoeia 9th Edition. Chapter 2.7.2, Microbiological Assay of Antibiotics. Strasbourg: Council of Europe, p. 240–275.
Falini G, Albeck S, Weiner S, Addadi L. 1996. Control of aragonite or calcite polymorphism by mollusk shell macromolecules. Science 271:67–69.
Folk RL. 1993. SEM imaging of bacteria and nanobacteria in carbonate sediments and rocks. J Sediment Petrol 63:990–999.
Forti P. 2002. Biogenic speleothems: an overview. IJS 30A(1/4):39–56.
Fu G, Valiyaveettil S, Wopenka B, Morse DE. 2005. $CaCO_3$ biomineralization: acidic 8-kDa proteins isolated from aragonitic abalone shell nacre can specifically modify calcite crystal morphology. Biomacromolecules 6:1289–1298.
Fujita Y, Ferris FG, Lawson RD, Colwell FS, Smith RW. 2000. Subscribed content calcium carbonate precipitation by ureolytic subsurface bacteria. Geomicrobiol J 17:305–318.
Geiss HK, Piotrowski HD, Hingst V. 1985. Evaluation of API 20 NE in routine diagnostics of nonfermenting gram-negative rod-shaped bacteria. Zentralbl Bakteriol Mikrobiol Hyg A 259:35–42.
González-Muñoz MT, Rodriguez-Navarro C, Martínez-Ruiz F, Arias JM, Merroun ML, Rodriguez-Gallego M. 2010. Bacterial biomineralization: new insights from Myxococcus-induced mineral precipitation. Geol Soc Spec Publ 336:31–50.
Griess P. 1879. Bemerkungen zu der abhandlung der H.H. Weselsky und Benedikt "Ueber einige azoverbindungen. Ber Dtsch Chem Ges 12:426–428.
Hammes F, Boon N, de Villiers J, Verstraete W, Siciliano SD. 2003. Strain-specific ureolytic microbial calcium carbonate precipitation. Appl Environ Microbiol 69:4901–4909.
Hasan HAH. 2000. Ureolytic microorganisms and soil fertility: a review. Commun Soil Sci Plant Anal 31(15–16):2565–2589.
Jones B. 2001. Microbial activity in caves – a geological perspective. Geomicrobiol J 18:345–313.
Jones B. 2010. In caves: agents of calcite corrosion and precipitation. In: Pedley HM, Rogerson M, editors. Tufas and speleothems: unravelling the microbial and physical controls. London: Geological Society Special Publications.
Kawaguchi T, Decho AW. 2002. A laboratory investigation of cyanobacterial extracellular polymeric secretion (EPS) in influencing $CaCO_3$ polymorphism. J Cryst Growth 240(1–2):230–235.
Kendall AC, Broughton PL. 1978. Origin of fabrics in speleothems composed of columnar calcite crystals. J Sediment Petrol 48:519–538.
Kim OS, Cho YJ, Lee K, Yoon SH, Kim M, Na H, Park SC, Jeon YS, Lee JH, Yi H, et al. 2012. Introducing EzTaxon-e: a prokaryotic 16S rRNA gene sequence database with phylotypes that represent uncultured species. Int J Syst Evol Microbiol 62:716–721.
Knorre H, Krumbein W. 2000. Bacterial calcification. In: Riding RE, Awramik SM, editors. Microbial sediments. Berlin, Germany: Springer-Verlag, p. 25–31.
Lane DJ, Pace B, Olsen GJ, Stahl DA, Sogin ML, Pace NR. 1985. Rapid determination of 16S ribosomal RNA sequences for phylogenetic analyses. Proc Natl Acad Sci USA 82:6955–6959.
Logan NA, Berkeley RCW. 1984. Identification of Bacillus strains using the API system. J Gen Microbiol 130:1871–1882.
Mantelli F, Menichetti S, Calà P. 2014. Principali emergenze termali in Toscana. Idrogeologia e chimica delle acque. ARPAT, Regione Toscana: Agenzia Regionale per la Protezione Ambientale della Toscana, p. 198–206.
McLean RJ, Beauchemin D, Beveridge TJ. 1992. Influence of oxidation state on iron binding by *Bacillus licheniformis* capsule. Appl Environ Microbiol 58:405–408.
Mobley HL, Hausinger RP. 1989. Microbial ureases: significance, regulation, and Molecular Characterization. Microbiol Mol Biol Rev 53:85–108.
Mulec J, Kosi G, Vrhovsek D. 2007. Algae promote growth of stalagmites and stalactites in karst caves (Skocjanske jame, Slovenia). Carbonates Evaporites 22:6–9.
Navarro-Gonzalvez JA, Garcıa-Benayas C, Arenas J. 1998. Semiautomated measurement of nitrate in biological fluids. Clin Chem 44:679–681.
Njegić-Džakula B, Brečević L, Falini G, Kralj D. 2011. Kinetic approach to biomineralization: interactions of synthetic polypeptides with calcium carbonate polymorphs. Croat Chem Acta 84:301–314.
Norris V, Grant S, Freestone P, Canvin J, Sheikh FN, Toth I, Trinei M, Modha K, Norman RI. 1996. Calcium signalling in bacteria. J Bacteriol 178:3677–3682.
Pacton M, Breitenbach SFM, Lechleitner FA, Vaks A, Rollion-Bard C, Gutareva OS, Osintcev AV, Vasconcelos C. 2013. The role of

microorganisms in the formation of a stalactite in Botovskaya Cave, Siberia – paleoenvironmental implications. Biogeosciences 10:6115–6130.
Paerl HW, Steppe TF, Reid RP. 2001. Bacterially mediated precipitation in marine stromatolites. Environ Microbiol 3:123–130.
Parkhurst DL. 1995. User's guide to PHREEQC–A computer program for speciation, reaction-path, advective-transport, and inverse geochemical calculations: U.S. Geological Survey Water-Resources Investigations Report 95-4227, 143 p.
Paulsen IT, Nguyen L, Sliwinski MK, Rabus R, Saier MH Jr. 2000. Microbial genome analyses: comparative transport capabilities in eighteen prokaryotes. J Mol Biol 301:75–100.
Pedley HM. 1994. Prokaryote-microphyte biofilms and tufas: a sedimentological perspective. Kaupia Darmstadter Beitr Nat 4:45–60.
Phillips AJ, Gerlach R, Lauchnor E, Mitchell AC, Cunningham AB, Spangler L. 2013. Engineered applications of ureolytic biomineralization: a review. Biofouling 29:715–733.
Piccini L. 2000. Il carsismo di origine idrotermale del Colle di Monsummano (Pistoia – Toscana). Le Grotte d'Italia 1:33–43.
Piciocchi A, Utili F. 1976. La Speleoterapia nella Grotta Giusti de Monsummano Terme. Annuario Speleologico C.A.I. Napoli 1974–1975. Napoli, Italy: Club Alpino Italiano - Sezione di Napoli, p. 91–98.
Pizzolante G, Cordero C, Tredici SM, Vergara D, Pontieri P, Del Giudice L, Capuzzo A, Rubiolo P, Kanchiswamy CN, Zebelo SA, et al. 2017. Cultivable gut bacteria provide a pathway for adaptation of *Chrysolina herbacea* to *Mentha aquatica* volatiles. BMC Plant Biol 17:30.
Rahman MA, Oomori T. 2008. Structure, crystallization and mineral composition of sclerites in the alcyonarian coral. J Cryst Growth 310:3528–3534.
Reffatti PF, Roy I, Odell M, Keshavarz T. 2013. Evidence for the involvement of intracellular Ca(2+) ions in the elicitation mechanism of *Bacillus licheniformis*. J Mol Microbiol Biotechnol 23:391–395.
Rodriguez-Navarro C, Jimenez-Lopez C, Rodriguez-Navarro A, Gonzalez-Munoz MT, Rodriguez-Gallego M. 2007. Bacterially mediated mineralization of vaterite. Geochim Cosmochim Acta 71:1197–1213.
Rodriguez-Navarro C, Jroundi F, Schiro M, Ruiz-Agudo E, González-Muñoz MT. 2012. Influence of substrate mineralogy on bacterial mineralization of calcium carbonate: implication for stone conservation. Appl Environ Microbiol 78:4017–4029.
Sambrook J, Russell D. 2001. Molecular Cloning: A Laboratory Manual. 3rd ed. New York: Cold Spring Harbor Laboratory Press.
Singh R, Yoon H, Sanford RA, Katz L, Fouke BW, Werth CJ. 2015. Metabolism-induced $CaCO_3$ biomineralization during reactive transport in a micromodel: Implications for porosity alteration. Environ Sci Technol 49:12094–12104.
Smith RJ. 1995. Calcium and bacteria. Adv Microb Physiol 3783–133.
Solomon CM, Collier JL, Berg GM, Glibert PM. 2010. Role of urea in microbial metabolism in aquatic systems: a biochemical and molecular review. Aquat Microb Ecol 5967–88.
Starkey RL. 1938. A study of spore formation and other morphological characteristics of Vibrio desulfuricans. Archiv Mikrobiol 9(1–5):268–304.
Sun Y, De Vos P, Heylen K. 2016. Nitrous oxide emission by the non-denitrifying, nitrate ammonifier *Bacillus licheniformis*. BMC Genomics 17:68.
Taylor MP, Drysdale RN, Carthew KD. 2004. The formation and environmental significance of calcite rafts in tropical tufa-depositing rivers of northern Australia. Sedimentology 51:1089–1101.
Tiano P, Biagiotti L, Mastromei G. 1999. Bacterial bio-mediated calcite precipitation for monumental stones conservation: methods of evaluation. J Microbiol Methods 36(1–2):139–145.
Tourney J, Ngwenya BT. 2009. Bacterial extracellular polymeric substances (EPS) mediate CaCO3 morphology and polymorphism. Chem Geol 262(3–4):138–146.
Vahabi A, Ramezanianpour AA, Sharafi H, Zahiri HS, Vali H, Noghabi KA. 2015. Calcium carbonate precipitation by strain *Bacillus licheniformis* AK01, newly isolated from loamy soil: a promising alternative for sealing cement-based materials. J Basic Microbiol. 55:105–111.
Vasconcelos C, McKenzie JA, Bernasconi S, Grujic D, Tien AJ. 1995. Microbial mediation as a possible mechanism for natural dolomite formation at low temperatures. Nature 377:220–222.
Versalovic JSM, De Bruijn FJ, Lupski JR. 1994. Genomic fingerprinting of bacteria using repetitive sequence-based polymerase chain reaction. Methods Mol Cell Biol 5:25–40.
Vigliotta G, Nutricati E, Carata E, Tredici SM, De Stefano M, Pontieri P, Massardo DR, Prati MV, De Bellis L, Alifano P. 2007. Clonothrix fusca Roze 1896, a filamentous, sheathed, methanotrophic gammaproteobacterium. Appl Environ Microbiol 73:3556–3565.
Waditee R, Hossain GS, Tanaka Y, Nakamura T, Shikata M, Takano J, Takabe T, Takabe T. 2004. Isolation and functional characterization of Ca^{2+}/H^{+} antiporters from Cyanobacteria. J Biol Chem 279:4330–4338.
[illegible]D, Côté JC. 2003. Phylogenetic relationships between *Bacillus* species and related genera inferred from comparison of 3' end 16S rDNA and 5' end 16S-23S ITS nucleotide sequences. Int J Syst Evol Microbiol 53(Pt 3):695–704.
Zamarreño DV, Inkpen R, May E. 2009. Carbonate crystals precipitated by freshwater bacteria and their use as a limestone consolidant. Appl Environ Microbiol 75:5981–5990.
Zavarzin GA. 2002. Microbial geochemical calcium cycle. Microbiology 71:1–17.
Zhu T, Dittrich M. 2016. Carbonate precipitation through microbial activities in natural environment, and their potential in biotechnology: a review. Front Bioeng Biotechnol 4:4.